

Syntheses, Structures, and Catalytic Ethylene Oligomerization Behaviors of Bis(phosphanyl)aminenickel(II) Complexes Containing *N*-Functionalized Pendant Groups

Keming Song,^[a,b] Haiyang Gao,^{*[a]} Fengshou Liu,^[a] Jin Pan,^[a] Lihua Guo,^[a] Shaobo Zai,^[a] and Qing Wu^{*[a,b]}

Keywords: Oligomerization / Nickel / Structure–activity relationships / P,P ligands

Several *N*-functionalized bis(phosphanyl)amine ligands respectively containing benzyl, furfuryl, thiophene-2-methyl, thiophene-2-ethyl, and 2-picoyl groups (**1a–e**) were synthesized and characterized. The ligands reacted with (DME)-NiBr₂ in CH₂Cl₂ to give their corresponding nickel complexes [Ph₂PN(R)PPh₂NiBr₂] [R = CH₂C₆H₅ (**2a**), CH₂C₄H₃O (**2b**), CH₂C₄H₃S (**2c**), CH₂C₅H₄N (**2d**), and CH₂CH₂C₄H₃S (**2e**)]. The structures of these complexes were established by single-crystal X-ray crystallography. All these nickel complexes were highly active towards ethylene oligomerization

in the presence of methylaluminoxane or Et₂AlCl, producing a high content of butene (C₄). Especially for **2e**, which contains a thiophene-2-ethyl pendant group, the oligomerization products obtained at –40 °C contained 95.9 mol-% C₄ fraction with 100 mol-% 1-butene. Over 50 °C, however, these nickel complexes underwent Friedel–Crafts alkylation of toluene with ethylene and the olefin oligomers.

(© Wiley-VCH Verlag GmbH & Co. KGaA, 69451 Weinheim, Germany, 2009)

Introduction

The oligomerization of ethylene is one of the major industrial processes for the production of α -olefins. These obtained oligomers can be used as comonomers in the polymerization of ethylene, plasticizers, and synthetic lubricants.^[1] Since the pioneering work of Keim and co-workers,^[2] nickel(II)-based catalysts with various chelating ligands such as N–N,^[3] O–P,^[4] P–N,^[5] and P–P^[6] have been extensively studied in the development of olefin oligomerization processes.

In the past decade, bis(phosphanyl)amines with P–N–P skeletons have been proved as much more versatile ligands, and varying the substituents on both the P and N centers gives rise to changes in the P–N–P angle and the conformation around the P centers.^[7] This feature enables the synthesis of a wide range of four-membered ring systems containing transition metals such as Pd, Pt, Mo, Cu, and Ru,^[8] which have potential uses in catalysis. In addition, a number of chromium complexes bearing the bis(phosphanyl)amine ligands with various substituents on both the N and P

atoms were studied as highly selective catalysts for ethylene trimerization and tetramerization.^[9] Wass and Jordan also reported that nickel complexes were efficient precatalysts for ethylene polymerization, producing high molecular-weight linear polyethylene.^[10] However, nickel complexes with these ligands are much less developed than chromium complexes. Moreover, the majority of structure/property correlation investigations for ethylene oligomerization or polymerization with bis(phosphanyl)amines nickel catalysts mainly focused on the influence of the P-donor moiety, especially bulky *ortho*-methoxy and 2-isopropyl groups in aryl phosphanes.^[10,11]

Recently, Bercaw^[12] and Hor^[13] synthesized chromium complexes containing bis(phosphanyl)amines with *N*-functionalized donor groups and found that the catalytic activity and catalyst lifetime was higher than those lacking an *N*-functionalized donor group on the ligand. Intensive studies showed that the nature of the functionalized donor would influence the catalytic activity and selectivity for olefin oligomerization.^[12–14] Therefore, we speculated that a bis(phosphanyl)amine with an *N*-functionalized donor group would be a potential hemilabile tridentate ligand and may provide stability to reactive intermediates or modify the transition states in the oligomerization catalysis.

In the work reported herein, we synthesized and characterized a series of new bis(phosphanyl)aminenickel(II) complexes by introducing an *N*-functionalized donor group. The effects of a functionalized donor on ethylene oligomerization behaviors were examined. In addition, the influences

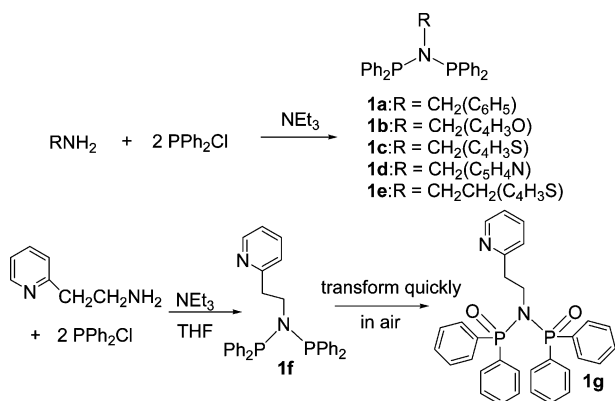
[a] DSAPM Lab, Institute of Polymer Science, School of Chemistry and Chemical Engineering, Sun Yat-sen (zhongshan) University, Guangzhou, 510275, P. R. China
Fax: +86-020-84114033
E-mail: ceswuq@mail.sysu.edu.cn
gaohy@mail.sysu.edu.cn

[b] PCFM Lab, OFCM Institute, Sun Yat-sen (zhongshan) University, Guangzhou, 510275, P. R. China

of the reaction temperature, Al/Ni molar ratio, and different co-catalysts on oligomerization activity and selectivity were also investigated in detail.

Results and Discussion

The *N*-functionalized pendant groups were designed for their potential ability to undergo reversible coordination to nickel metal. The addition of a functional pendant at the N-site would raise the denticity and coordinative flexibility of these ligands. The donor functionality is represented by benzyl (**1a**), furfuryl (**1b**), thiophene-2-methyl (**1c**), 2-picolyl (**1d**), and thiophene-2-ethyl (**1e**), ranging from weak to moderate basicity. These new *N*-donor-functionalized bis(phosphanyl)amine ligands were prepared from a functionalized primary amine by classical aminolysis with Ph_2PCl in a one-step reaction (49–67.5% yield; Scheme 1).^[15] All of the products showed a single resonance in their ^{31}P NMR spectra that lied in the expected region of 60–70 ppm,^[16] suggesting that both phosphorus atoms were chemically equivalent in solution. The chemical shifts of compounds **1b–e** were shifted downfield with respect to that of compound **1a**, and **1e** had the lowest field resonance at $\delta = 63.25$ ppm. Compounds **1a–e** could be crystallized from ethanol in air and were stable in the solid state, but they underwent slow decomposition and oxidation in solution.^[17]



Scheme 1. Preparation of ligands **1a–e** and **1g**.

However, it was found that ligand **1f** (see Scheme 1) was transformed into oxide **1g** during purification by column chromatography in air. This can be attributed to the prolonged exposure of the ligand solution to air. The structure of ligand **1g** was established by single-crystal X-ray crystallography (Figure 1), and it was found that the P–N–P skeleton with a pyridyl-2-ethylene side chain extended from the N-site.

Complexations between $(\text{DME})\text{NiBr}_2$ and ligands **1a–e** in CH_2Cl_2 occurred readily at room temperature (Scheme 2). All the complexes were stable and much less sensitive to moisture and oxygen. The structures of the complexes were confirmed by elemental analysis, NMR spectroscopy, and X-ray data. The ^{31}P NMR spectra of **2a–e** respectively displayed a singlet at $\delta = 52.47$ ppm for

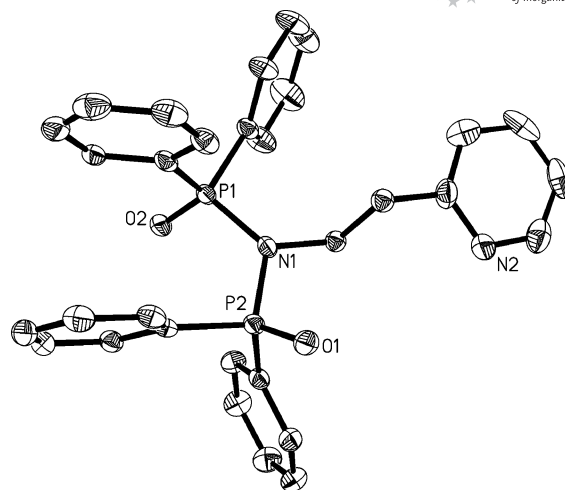
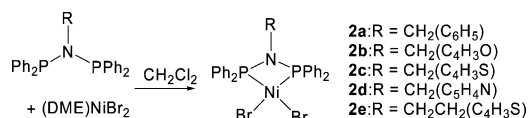


Figure 1. Molecular structure of **1g**. Hydrogen atoms are omitted for clarity. Selected bond lengths [Å] and angles [°]: P1–O2 1.4714(19), P1–N1 1.689(2), P2–O1 1.4766(19), P2–N1 1.691(2), O2–P1–N1 112.60(11), O1–P2–N1 112.02(11), P1–N1–P2 124.11(12).

2a, 51.30 ppm for **2b**, 52.36 ppm for **2c**, 52.33 ppm for **2d**, and 48.85 ppm for **2e**. It is interesting to note that the ^{31}P NMR chemical shift of **2a** was nearly identical to those of compounds **2c** and **2d**, despite the presence of the thienyl and pyridyl group in the latter complexes. This result indicated that the pyridyl or thienyl group had little or no electronic influence on the phosphorus center.



Scheme 2. Syntheses of bis(phosphanyl)aminenickel(II) complexes **2a–e**.

Crystals of nickel complexes **2a–e** suitable for X-ray crystallography were grown from CH_2Cl_2 /hexane or CH_2Cl_2 solutions. ORTEP diagrams are shown in Figures 2, 3, 4, 5, and 6 along with selected bond lengths and bond angles, respectively.

All five complexes adopt a square-planar coordination at the nickel atom and a near-planar four-membered chelate ring (NiP_2N), similar to previously reported bis(phosphanyl)amine nickel complexes.^[10,18] However, the pendant donors are located away from the metal and do not show any bonding interaction with the nickel metal center in both the solid state and solution, even the 2-picolyl (**2d**) and thiophene-2-ethyl (**2e**), like those bis(phosphanyl)amine Pd, Pt, and Cr complexes reported elsewhere.^[12–13,17]

In general, the bond lengths and angles of **2a–e** in the solid state were very similar, with minimal structural differences due to the different functional groups. The shortest Ni–P bond length was given in complex **2d** [2.1161(13) Å]. Similarly, their P–N bond lengths were within expected values in comparison to the aminophosphane transition-metal structures.^[19] The two bite angles (P–N–P and P–Ni–P) of all the complexes were nearly the same. The P–N–P angles

ranged from 96.36(12) (for **2e**) to 98.0(2)° (for **2c**) and the P–Ni–P angles lied in the range 73.39(3)–73.80(5)°. In comparison to those sterically encumbered chelates PNP–Ni complexes [P–N–P 92.49(7)°; Ni–P 2.1611(6) Å],^[10a] the relatively slight increase in the P–N–P angle [96.36(12)° for **2e**; 98.0(2)° for **2c**] appeared along with a decrease in the Ni–P bond lengths [2.1161(13) Å for **2d**; 2.1347(16) Å for **2c**]. The shorter Ni–P bond length and the more open interspace of these complexes may afford more stable nickel species and space for the insertion of ethylene during oligomerization, which may explain why these nickel(II) bis(phosphanyl) amine complexes were effective catalyst precursors for ethylene oligomerization.

Ethylene oligomerization was carried out with these nickel complexes in the presence of methylaluminoxane (MAO) or Et₂AlCl. The results of oligomerization reactions

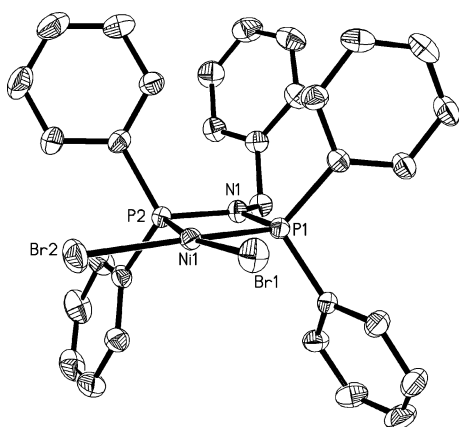


Figure 2. Molecular structure of **2a**. Hydrogen atoms and the CH₂Cl₂ molecule are omitted for clarity. Selected bond lengths [Å] and angles [°]: Ni1–P1 2.1238(10), Ni1–P2 2.1274(10), Ni1–Br1 2.3314(6), Ni1–Br2 2.3193(6), P1–Ni1–P2 73.60(4), P2–Ni1–Br2 94.02(3), P1–Ni1–Br1 93.60(3), Br2–Ni1–Br1 99.04(2), P1–Ni1–P2 97.61(14).

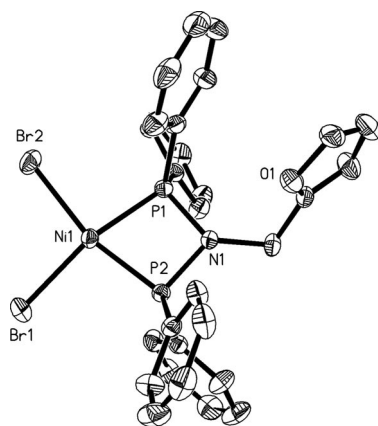


Figure 3. Molecular structure of **2b**. Hydrogen atoms are omitted for clarity. Selected bond lengths [Å] and angles [°]: Ni1–P1 2.1278(8), Ni1–P2 2.1285(8), Ni1–Br1 2.3284(6), Ni1–Br2 2.3312(5), P1–N1 1.692(2), P2–N1 1.696(2), P1–Ni1–P2 73.74(3), P2–Ni1–Br1 94.61(3), P1–Ni1–Br2 92.19(3), Br1–Ni1–Br2 99.61(2), P1–Ni1–P2 97.83(11).

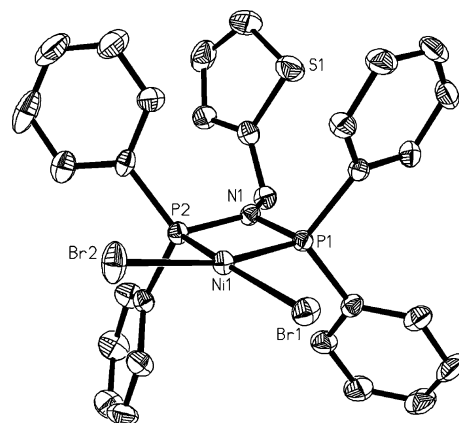


Figure 4. Molecular structure of **2c**. Hydrogen atoms are omitted for clarity. Selected bond lengths [Å] and angles [°]: Ni1–P1 2.1185(15), Ni1–P2 2.1347(16), Ni1–Br2 2.3225(10), Ni1–Br1 2.3306(10), P1–N1 1.685(5), P2–N1 1.685(4), P1–Ni1–P2 73.47(6), P2–Ni1–Br2 94.49(5), P1–Ni1–Br1 91.81(5), Br2–Ni1–Br1 101.29(4), P2–N1–P1 98.0(2).

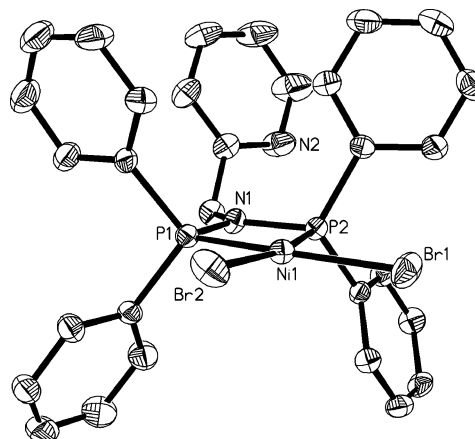


Figure 5. Molecular structure of **2d**. Hydrogen atoms and the CH₂Cl₂ molecule are omitted for clarity. Selected bond lengths [Å] and angles [°]: Ni1–P1 2.1161(13), Ni1–P2 2.1282(13), Ni1–Br2 2.3229(8), Ni1–Br1 2.3241(8), P1–Ni1–P2 73.80(5), P1–Ni1–Br2 93.23(4), P2–Ni1–Br1 93.71(4), Br2–Ni1–Br1 99.38(3), P1–Ni1–P2 97.70(18).

conducted at 20 °C and atmospheric pressure are summarized in Table 1. All the catalysts were highly active for ethylene oligomerization with catalytic activities over 10⁵ g ethylene/(mol Ni h) and no polymer was found in the products. GC–MS analyses confirmed that the products mainly consisted of C₄ (butene) as well as a small amount of C₆ (hexene) oligomers. Generally, all the bis(phosphanyl) aminenickel complexes were highly active ethylene dimerization precursors. Compared to [ArPN(Me)PAR]NiBr₂ nickel complexes reported by Wass,^[10a,20] the bis(phosphanyl)aminenickel complexes containing an *N*-functionalized pendant group showed higher catalytic activity.

The structures of the nickel complexes influenced their catalytic activities. The activity increased in the order of increasing basicity of the *N*-functionalized pendant group:

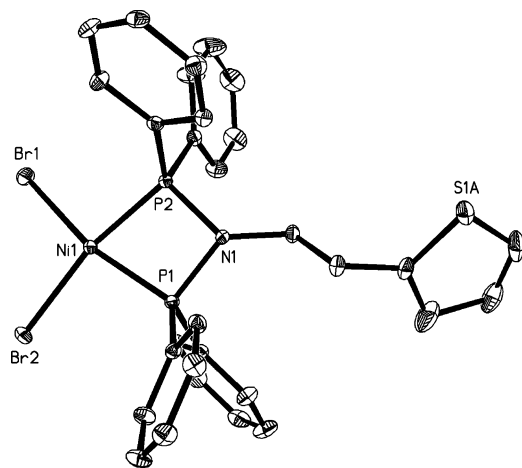


Figure 6. Molecular structure of **2e**. Hydrogen atoms and the CH_2Cl_2 molecule are omitted for clarity. Selected bond lengths [Å] and angles [°]: Ni1–P2 2.1198(8), Ni1–P1 2.1245(8), Ni1–Br1 2.3261(5), Ni1–Br2 2.3283(5), P2–Ni1–P1 73.39(3), P2–Ni1–Br1 95.42(3), P1–Ni1–Br2 93.56(3), Br1–Ni1–Br2 98.088(19), P2–Ni1–P1 96.36(12).

2a < **2b** < **2c** < **2d**, which indicates that introduction of a Lewis base group favors ethylene insertion. However, the order of the selectivity was different from that of activity. As shown in Table 1, complex **1a** has the lowest selectivity for C4 among complexes **2a–d**, suggesting that introduction of *N*-functionalized pendant groups can increase oligomerization selectivity. Complex **2d** with a 2-picoyl group had relatively low selectivity (78.8%) for C4, although it showed the highest catalytic activity. The selectivity for C4 (87.4%) and 1-C4 (61.8%) of complex **2b** with a furan-pendant group was the highest. A reasonable explanation for the catalytic activity enhancement and selectivity increase is that the *N*-functionalized moieties may coordinate to the nickel center after complexes **2b**, **2c**, and **2d** are activated by MAO, and this coordination may also make the formation of the nickel species much more favorable for ethylene insertion and selective for dimerization of ethylene. Similar results had also been reported for Ti and Co complexes with a thiophene pendant group, and DFT modeling studies showed that the thienyl sulfur atom or pyridyl nitrogen atom had coordination interaction to the metal center.^[21]

Varying the length of the pendant group also had an effect on catalyst activity. Catalyst **2e** containing a thiophene-2-ethyl group was less active than analogue **2c** containing a thiophene-2-methyl group. On the contrary, the selectivity for linear α -olefins (1-C4 and 1-C6) increased substantially with increasing the pendant length. Moreover, the selectivity for α -olefins and C4 would increase obviously in the presence of a longer thiophene group, which may result from easy coordination interaction of the thienyl sulfur atom of **2e** to nickel.^[21]

The choice of aluminum co-catalyst also has a significant effect on the ethylene oligomerization reactions. Activation of the nickel complexes with Et_2AlCl instead of MAO made the catalysts much more active, and a higher proportion of C4 was obtained. As compared with the MAO system (Table 1, Entry 4), the catalytic activity of **2d** activated by Et_2AlCl (Table 1, Entry 7) increased twofold and the C4 content increased from 78.8 to 98.5%. However, the selectivity for the α -olefins decreased markedly, suggesting that MAO was an effective co-catalyst to restrict olefin isomerization for these P–N–P nickel complexes. Similar oligomerization results were recently observed in nickel catalysts chelating tridentate pyrazolyl ligands.^[22]

Considering these nickel complex/MAO catalytic systems would oligomerize ethylene with better selectivity for α -olefins, MAO was selected as a practical activator to probe the effects of reaction parameters such as temperature and Al/Ni molar ratio on ethylene oligomerization. The oligomerization results are shown in Table 2.

The reaction temperature strongly affected the catalytic activities. With an increase in temperature from -40 to 50 °C, the catalytic activities reached a maximum value at 20 °C for **2a–c** and -15 °C for **2e**, whereas for **2d** the catalytic activity decreased continuously. It is noteworthy that for all these catalytic systems, elevating the reaction temperature to 50 °C led to a remarkable reduction in activity (Table 2, Entries 5, 10, 15, 20), which may be ascribed to the decomposition of the active catalytic sites and lower ethylene solubility at high temperature.^[23] Variation of the reaction temperature also influenced the distribution of the products. As the temperature was increased, the proportion of C4 and selectivity for 1-C4 and linear 1-C6 decreased consistently. All the nickel complex/MAO systems showed

Table 1. Ethylene oligomerization catalyzed by **2a–e**/MAO or Et_2AlCl .^[a]

Entry	Complex	Co-catalyst	Al/Ni	Activity ^[b]	Oligomer product distribution ^[c] [mol-%]			
					C4	C6	1-C4	1-C6
1	2a (R = benzyl)	MAO	400	2.81	76.9	23.1	48.9	13.2
2	2b (R = furfuryl)	MAO	400	3.04	87.4	12.6	61.8	24.3
3	2c (R = thiophene-2-methyl)	MAO	400	3.19	84.6	15.4	34.7	7.81
4	2d (R = 2-picoyl)	MAO	400	3.57	78.8	21.2	22.5	8.57
5	2e (R = thiophene-2-ethyl)	MAO	400	2.05	88.3	11.7	58.9	27.8
6	2a (R = benzyl)	Et_2AlCl	200	5.62	83.5	16.5	11.3	2.9
7	2d (R = 2-picoyl)	Et_2AlCl	200	6.84	98.5	1.5	3.44	1.31

[a] Oligomerization conditions: 20 °C, 30 min, toluene (30 mL), complex (10 μmol), ethylene pressure (0.5 atm); MAO as co-catalyst.

[b] 10^5 g ethylene/(mol Ni h). [c] Determined by GC–MS.

Table 2. Ethylene oligomerization catalyzed by **2a–e**/MAO at different temperatures and Al/Ni molar ratios.^[a]

Entry	Complex	Al/Ni	T [°C]	Activity ^[b]	Oligomer product distribution ^[c] [mol-%]			
					C4	C6	1-C4	1-C6
1	2a	400	−40	1.48	94.5	5.5	98.2	75.3
2	2a	400	−15	2.74	89.5	10.5	90.6	47.0
3	2a	400	0	2.74	86.8	13.2	67.2	21.8
4	2a	400	20	2.81	76.9	23.1	48.9	13.2
5 ^[d]	2a	400	50	0.84				
6	2b	400	−40	1.60	92.0	8.0	99.5	92.4
7	2b	400	−15	1.75	90.1	9.9	90.7	57.8
8	2b	400	0	2.74	88.5	11.5	73.2	34.3
9	2b	400	20	3.04	87.4	12.6	61.8	24.3
10 ^[d]	2b	400	50	0.85				
11	2c	400	−40	1.52	93.2	6.8	98.6	88.4
12	2c	400	−15	2.20	90.3	9.7	88.8	49.9
13	2c	400	0	2.59	90.2	9.8	64.7	23.5
14	2c	400	20	3.19	84.6	15.4	34.7	7.81
15 ^[d]	2c	400	50	1.52				
16	2d	400	−40	5.78	87.4	12.6	92.3	58.7
17	2d	400	−15	4.18	80.2	19.8	73.3	36.9
18	2d	400	0	3.88	72.6	27.4	55.7	29.8
19	2d	400	20	3.57	78.8	21.2	22.5	8.57
20 ^[d]	2d	400	50	2.28				
21	2e	400	−40	2.58	95.9	4.1	100	94.3
22	2e	400	−15	3.27	90.9	9.1	91.4	58.2
23	2e	400	0	2.58	90.8	9.2	71.6	36.3
24	2e	400	20	2.05	88.3	11.7	58.9	27.8
25 ^[d]	2e	400	50	1.00				
26	2a	200	20	2.58	76.5	23.5	54.8	16.0
27	2a	800	20	1.82	84.7	15.3	56.9	17.4
28	2d	200	20	2.89	78.3	21.7	30.8	15.6
29	2d	800	20	2.96	80.0	20.0	31.6	15.3

[a] Oligomerization conditions: 30 min, toluene (30 mL), complex (10 μ mol), ethylene pressure (0.5 atm), MAO as co-catalyst. [b] 10^5 g ethylene/(mol Ni h). [c] Determined by GC–MS. [d] Alkyltoluenes were the main products, and only trace amounts of ethylene oligomers were detected.

similar evolution. These results indicated that the rate of chain isomerization relative to that of chain transfer increased with increasing temperature. Because ethylene solubility in toluene would decrease with increasing temperature,^[24] the loss of the selectivity for α -olefins with increasing temperature could be partly due to lower concentrations of ethylene in solution.^[25] At −40 °C, a very high C4 content (95.9%) and selectivity of 1-C4 (100%) were detected for the **2e**/MAO system. Typical GC–MS analyses of the ethylene oligomers obtained by **2e**/MAO at different temperatures are shown in Figure 7.

In addition, it should be pointed out that ethylene consumption could only be observed in the first 2 min for **2a–e**/MAO at 50 °C, indicating the fast decomposition of active species at higher temperature. Surprisingly, at the elevated temperature, alkyltoluenes were the main products, and only trace amounts of oligomers were observed, which was absolutely different from the products obtained at lower temperature. The details of the alkylation products are discussed below.

The effects of various Al/Ni ratios on ethylene oligomerization were also investigated by using the **2a**/MAO and **2d**/MAO systems. As shown in Table 2, the experimental results for ethylene oligomerization with a change in Al/Ni molar ratio in the range from 200 to 800 at 20 °C showed that the Al/Ni mole ratio had only a slight effect on the

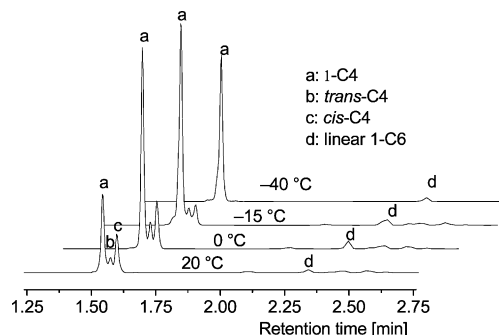


Figure 7. GC–MS analyses of ethylene oligomers obtained by **2e**/MAO at different temperatures (Table 2, Entry 21–24).

catalytic activity and distribution of the oligomers, suggesting that it was not a dominant parameter controlling the oligomerization.

As mentioned above, increasing the temperature to 50 °C led to a quite different set of products. As shown in Figure 8, GC–MS analyses confirmed that the products obtained from **2a**/MAO and **2d**/MAO at 50 °C consisted of C2 (**A**, **C**, **E**), C4 (**B**), and C6 (**D**) alkyl-substituted toluenes, each as a mixture of regioisomers. The alkylation products could be generated from Friedel–Crafts reaction between ethylene or its oligomers and the toluene solvent.^[26] Very

recently, nickel complexes bearing [N,P]-five-membered chelating rings were reported to catalyze reactions with ethylene producing oligomers and alkylated toluenes.^[27]

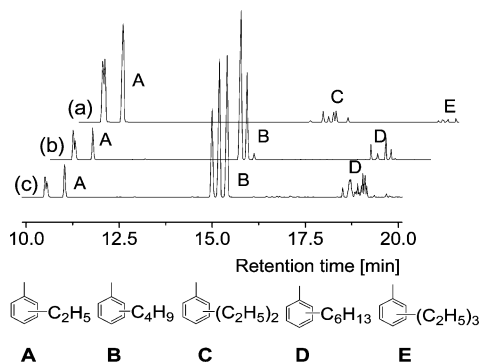


Figure 8. GC-MS analyses of products obtained with (a) AlCl_3 (Table 3, Entry 5), (b) **2a**/MAO (Table 3, Entry 1), and (c) **2d**/MAO (Table 3, Entry 2).

To further understand the Friedel–Crafts reaction in such systems, **2a**, **2d**, MAO, AlCl_3 , and NiBr_2/MAO were independently tested under identical conditions at 50 °C and the results were compared with those obtained for the **2a**/MAO and **2d**/MAO systems. As shown in Table 3, when MAO or nickel complexes **2a** or **2d** was used alone, neither ethylene oligomerization nor the Friedel–Crafts reaction was catalyzed, whereas AlCl_3 , as a strong Lewis acid, could typically catalyze the Friedel–Crafts reaction of ethylene with toluene to produce C2-alkyl toluenes (**A**, **C**, and **E**).^[28] In addition, with the use of NiBr_2/MAO , neither ethylene consumption nor alkylated product was observed, suggesting that the ligand was also an indispensable factor in the initiation of the Friedel–Crafts reaction in the present catalytic systems.

Until now, there have been only a few reports on the mechanism of formation of the real active species for toluene alkylation in nickel complex/MAO catalytic systems. According to our experimental results, we can presume that the active species for ethylene oligomerization decomposes rapidly at high temperature and transforms into a new strong Lewis acid. The mechanism for the acid-catalyzed alkylation of toluene involves ethylene or the produced oligomer protonated at the acidic sites. Subsequently, the protonated species (carbocation precursor) can react with toluene to produce the alkyl-substituted toluenes.^[26a,28]

Conclusions

We successfully synthesized and characterized a series of new bis(phosphanyl)amine ligands containing an *N*-functionalized pendant group and their corresponding nickel complexes. All the complexes are four-coordinate and have a near-planar geometry at the nickel center. In the presence of MAO or Et_2AlCl , the nickel complexes showed high activity for ethylene oligomerization, and the products obtained were mainly dimers, with a small amount of trimer with a high selectivity for linear α -olefins. However, a higher selectivity for α -olefins (1-C4 or 1-C6) was obtained when activated by MAO rather than Et_2AlCl . Both the catalytic activity and selectivity for α -olefin oligomers were mostly dependent on the structure of the complexes and the reaction temperatures. Moreover, the activity increased in the order of increasing basicity of *N*-functionalized pendant ligand: **2a** < **2b** < **2c** < **2d**. The catalysts afforded a higher C4 content and better selectivity for linear α -olefins with decreasing reaction temperature. Especially for complex **2e** with a thiophene-2-ethyl pendant group, the oligomerization products containing 95.9 mol-% C4 fraction with 100 mol-% 1-butene were obtained at –40 °C. However, at elevated temperatures (50 °C), the nickel complex/MAO systems decomposed rapidly and underwent Friedel–Crafts alkylation of toluene with ethylene and the olefin oligomers.

Experimental Section

General Methods: All manipulations involving air- and moisture-sensitive compounds were carried out under an atmosphere of dried and purified nitrogen by using standard Schlenk and vacuum-line techniques. Toluene, hexane, and THF were dried with sodium metal and distilled under an atmosphere of nitrogen; dichloromethane was dried with P_2O_5 and distilled under an atmosphere of nitrogen. $(\text{DME})\text{NiBr}_2$ was synthesized by the reaction of 1,2-dimethoxyethane with anhydrous nickel(II) bromide, according to the report in the literature.^[29] Methylaluminoxane (MAO) was prepared by partial hydrolysis of trimethylaluminum (TMA) in toluene at 0–60 °C with $\text{Al}_2(\text{SO}_4)_3 \cdot 18\text{H}_2\text{O}$ as the water source. The initial $[\text{H}_2\text{O}]/[\text{TMA}]$ molar ratio was 1.3. Diethylaluminum chloride (Et_2AlCl) was obtained from the Institute of Chemical Engineering (Shanghai) and diluted to 350 g/L solutions in *n*-heptane prior to use. Anhydrous Ni^{II} bromide (99%), benzylamine (98%), diphenylphosphane chloride (95%), furfurylamine, thiophene-2-methylamine, 2-(aminomethyl)pyridine, thiophene-2-ethylamine, and 2-

Table 3. The data of alkylation in toluene.^[a]

Entry	Complex	MAO [mmol]	Activity ^[b]	Alkylation products ^[c] [mol-%]				
				A	B	C	D	E
1	2a	4	0.84	19.0	71.4	0	9.6	0
2	2d	4	2.28	11.1	71.9	trace	11.0	0
3	2a	0	0	–	–	–	–	–
4	2d	0	0	–	–	–	–	–
5	AlCl_3	0	0.69	86.3	0	11.0	0	2.7
6	NiBr_2	4	0	–	–	–	–	–
7	–	4	0	–	–	–	–	–

[a] Reaction conditions: 50 °C, 30 min, toluene (30 mL), complex (10 μmol), ethylene pressure (0.5 atm). [b] 10^5 g ethylene/(mol Ni h). [c] Determined by GC–MS (see Figure 8).

(aminoethyl)pyridine were bought from Alfa Aesar Co. and used without further purification. Other commercially available reagents were purchased and used without purification.

Measurement: Elemental analyses were performed with a Vario EL microanalyzer. ^1H NMR spectra were recorded with an INOVA 300 MHz instrument at room temperature in CDCl_3 solution for ligands and an INOVA 400 MHz instrument at room temperature in CDCl_3 solution for complexes, respectively, with tetramethylsilane as external standard. The chemical shifts for ^{31}P NMR spectra are reported in ppm at 121 MHz for ligands and 161.97 MHz for complexes, with 85% H_3PO_4 as external standard. The GC–MS data were recorded with a Finnigan Voyager GC-8000 TOP series GC–MS system with DB-5MS GC column. The following temperature program of the oven was adopted: 40 °C for 2 min, the temperature was increased by 5 °C/min heating to 110 °C, and then the temperature was increased by a 15 °C/min heating until 250 °C; this value was kept constant for a further 2 min.

Syntheses of Ligands and Complexes

$\text{C}_6\text{H}_5\text{CH}_2\text{N}(\text{PPh}_2)_2$ (1a**):** To a mixture of benzylamine (1.15 mL, 10.5 mmol) and triethylamine (4.16 mL, 30 mmol) in THF (70 mL) at 0 °C was added a solution of diphenylphosphane chloride (4 mL, 22 mmol) in THF (10 mL). The resulting solution was stirred for 20 h, after which the suspension was filtered through a layer of Celite to remove the triethylammonium salt formed. Removal of the solvent gave a pale-yellow oil. Crystallization from a concentrated ethanol solution at –20 °C yielded 3.12 g (6.57 mmol, 62.4%) of $\text{C}_6\text{H}_5\text{CH}_2\text{N}(\text{PPh}_2)_2$ (**1a**) as colorless crystals.^[15] $\text{C}_{31}\text{H}_{27}\text{NP}_2$ (475.5): calcd. C 78.30, H 5.72, N 2.95; found C 78.12, H 5.73, N 2.94. ^1H NMR (300 MHz, CDCl_3): δ = 7.40–7.35 (m, 8 H), 7.33–7.26 (m, 12 H), 7.14–7.07 (m, 3 H), 6.80–6.76 (m, 2 H), 4.55–4.48 (t, 2 H) ppm. ^{31}P NMR (121 MHz, CDCl_3): δ = 60.37(s) ppm.

$\text{C}_4\text{H}_3\text{OCH}_2\text{N}(\text{PPh}_2)_2$ (1b**):** Colorless crystals of **1b** were prepared according to a similar method described for **1a** in 55.4% yield. $\text{C}_{29}\text{H}_{25}\text{NOP}_2$ (465.46): calcd. C 74.83, H 5.41, N 3.01; found C 74.92, H 5.45, N 2.95. ^1H NMR (300 MHz, CDCl_3): δ = 7.38–7.30 (m, 8 H), 7.29–7.21 (m, 12 H), 7.09 (m, 1 H), 6.07 (m, 1 H), 5.43 (d, 1 H), 4.33–4.27 (t, 2 H) ppm. ^{31}P NMR (121 MHz, CDCl_3): δ = 63.24 (s) ppm.

$\text{C}_4\text{H}_3\text{SCH}_2\text{N}(\text{PPh}_2)_2$ (1c**):** Colorless crystals of **1c** were prepared according to a similar method described for **1a** in 57.8% yield. $\text{C}_{29}\text{H}_{25}\text{NSP}_2$ (481.53): calcd. C 72.33, H 5.23, N 2.91; found C 72.60, H 5.25, N 2.82. ^1H NMR (300 MHz, CDCl_3): δ = 7.36–7.30 (m, 8 H), 7.28–7.24 (m, 12 H), 7.00 (m, 1 H), 6.71 (m, 1 H), 6.40 (d, 1 H), 4.63–4.56 (t, 2 H) ppm. ^{31}P NMR (121 MHz, CDCl_3): δ = 62.68 ppm.

$\text{C}_5\text{H}_4\text{NCH}_2\text{N}(\text{PPh}_2)_2$ (1d**):** Colorless crystals of **1d** were prepared according to a similar method described for **1a** in 67.5% yield. $\text{C}_{30}\text{H}_{26}\text{N}_2\text{P}_2$ (476.49): calcd. C 75.62, H 5.50, N 5.88; found C 75.50, H 5.52, N 5.92. ^1H NMR (300 MHz, CDCl_3): δ = 8.40 (m, 1 H), 7.44–7.38 (m, 8 H), 7.31 (m, 1 H), 7.29–7.25 (m, 12 H), 6.96 (m, 1 H), 6.65 (d, 1 H), 4.70–4.63 (t, 2 H) ppm. ^{31}P NMR (121 MHz, CDCl_3): δ = 62.58 (s) ppm.

$\text{C}_4\text{H}_3\text{SCH}_2\text{CH}_2\text{N}(\text{PPh}_2)_2$ (1e**):** Colorless crystals of **1e** were prepared according to a similar method described for **1a** in 49.2% yield. $\text{C}_{30}\text{H}_{27}\text{NP}_2\text{S}$ (495.55): calcd. C 72.71, H 5.49, N 2.83; found C 73.01, H 5.58, N 2.72. ^1H NMR (300 MHz, CDCl_3): δ = 7.42 (m, 8 H), 7.33 (m, 12 H), 6.98 (s, 1 H), 6.77 (s, 1 H), 6.41 (m, 1 H), 3.49–3.46 (m, 2 H), 2.48–2.42 (m, 2 H) ppm. ^{31}P NMR (121 MHz, CDCl_3): δ = 63.25 (s) ppm.

$\text{C}_5\text{H}_4\text{NCH}_2\text{CH}_2\text{N}(\text{OPh})_2$ (1g**):** To a mixture of 2-(aminoethyl)pyridine (1.5 mL, 12.52 mmol) and triethylamine (5.6 mL,

40 mmol) in THF (70 mL) at 0 °C was added a solution of diphenylphosphane chloride (5.04 mL, 28 mmol) in THF (10 mL). The resulting solution was stirred for 20 h, and then the suspension was filtered through a layer of Celite to remove the triethylammonium salt formed. Removal of the solvent gave **1f** as a pale-yellow oil. The crude product was purified by column chromatography (hexane/ethyl acetate, 1:4) in air to afford exclusively the corresponding oxide **1g**. Crystallization from a concentrated ethanol solution at –20 °C yielded colorless crystals (3.6 g). $\text{C}_{31}\text{H}_{28}\text{N}_2\text{O}_2\text{P}_2$ (522.51): calcd. C 71.26, H 5.40, N 5.36; found C 71.42, H 5.48, N 5.28. ^1H NMR (300 MHz, CDCl_3): δ = 8.26 (s, 1 H), 7.85–7.79 (t, 8 H), 7.45–7.28 (m, 13 H), 6.96–6.94 (m, 1 H), 6.60–6.58 (m, 1 H), 3.75–3.70 (m, 2 H), 2.92–2.89 (m, 2 H) ppm. ^{31}P NMR (121 MHz, CDCl_3): δ = 30.17 (s) ppm.

$\text{C}_6\text{H}_5\text{CH}_2\text{N}(\text{PPh}_2)_2\text{NiBr}_2$ (2a**):** Bis(phosphanyl)aminenickel(II) complex **2a** was prepared by using a similar published procedure.^[10b] A solution of $\text{C}_6\text{H}_5\text{CH}_2\text{N}(\text{PPh}_2)_2$ (**1a**; 580 mg, 1.22 mmol) in CH_2Cl_2 (20 mL) was added to a solution of (DME)- NiBr_2 (415 mg, 1.34 mmol) in CH_2Cl_2 (10 mL). The mixture turned dark red. The mixture was stirred overnight, after which it was filtered through a layer of Celite to remove the superfluous (DME)- NiBr_2 . The solution was concentrated to ca. 5 mL by evaporation under reduced pressure and addition of *n*-hexane (30 mL) gave a brick-red solid powder. Product **2a** was collected by suction filtration and dried in vacuo. Yield: 715 mg, 84.4%. The complex was dissolved in CH_2Cl_2 /hexane at room temperature, and then slow diffusion under an atmosphere of nitrogen over one week gave crystals suitable for X-ray crystallography. $\text{C}_{31}\text{H}_{27}\text{Br}_2\text{NNiP}_2$ (694.0): calcd. C 53.65, H 3.92, N 2.02; found C 53.92, H 3.95, N 1.99. ^1H NMR (400 MHz, CDCl_3): δ = 7.90–7.87 (m, 8 H), 7.65–7.61 (t, 4 H), 7.50–7.47 (t, 8 H), 7.08–7.05 (t, 1 H), 6.90–6.86 (t, 2 H), 6.39–6.37 (d, 2 H), 3.93–3.87 (t, 2 H) ppm. ^{31}P NMR (161.97 MHz, CDCl_3): δ = 52.47 (s) ppm.

$\text{C}_4\text{H}_3\text{OCH}_2\text{N}(\text{PPh}_2)_2\text{NiBr}_2$ (2b**):** By using a similar method as adopted above, a mixture of **1b** (520 mg, 1.12 mmol) and (DME)- NiBr_2 (380 mg, 1.23 mmol) gave **2b** (623 mg, 81.3% yield) as a brick-red solid. The complex was dissolved in CH_2Cl_2 at room temperature, and then slow diffusion under an atmosphere of nitrogen over one week gave crystals suitable for X-ray crystallography. $\text{C}_{29}\text{H}_{25}\text{Br}_2\text{NNiOP}_2$ (683.96): calcd. C 50.93, H 3.68, N 2.05; found C 51.20, H 3.71, N 2.15. ^1H NMR (400 MHz, CDCl_3): δ = 7.93–7.87 (m, 8 H), 7.63–7.59 (m, 4 H), 7.51–7.47 (m, 8 H), 6.90–6.89 (m, 1 H), 6.02–6.00 (m, 1 H), 5.62–5.61 (d, 1 H), 3.78–3.73 (t, 2 H) ppm. ^{31}P NMR (161.97 MHz, CDCl_3): δ = 51.30 (s) ppm.

$\text{C}_4\text{H}_3\text{SCH}_2\text{N}(\text{PPh}_2)_2\text{NiBr}_2$ (2c**):** By using a similar method as adopted above, a mixture of **1c** (585 mg, 1.22 mmol) and (DME)- NiBr_2 (412 mg, 1.34 mmol) gave **2c** (700 mg, 82% yield) as a brick-red solid. The complex was dissolved in CH_2Cl_2 at room temperature and then slow diffusion under an atmosphere of nitrogen over one week gave crystals suitable for X-ray crystallography. $\text{C}_{29}\text{H}_{25}\text{Br}_2\text{NNiSP}_2$ (700.03): calcd. C 49.76, H 3.60, N 2.00; found C 50.01, H 3.71, N 1.91. ^1H NMR (400 MHz, CDCl_3): δ = 7.91–7.86 (m, 8 H), 7.66–7.62 (m, 4 H), 7.53–7.47 (m, 8 H), 7.98–7.96 (m, 1 H), 6.60–6.57 (m, 1 H), 6.21–6.20 (d, 1 H), 4.09–4.03 (t, 2 H) ppm. ^{31}P NMR (161.97 MHz, CDCl_3): δ = 52.36 (s) ppm.

$\text{C}_5\text{H}_4\text{NCH}_2\text{N}(\text{PPh}_2)_2\text{NiBr}_2$ (2d**):** By using a similar method as adopted above, a mixture of **1d** (542 mg, 1.14 mmol) and (DME)- NiBr_2 (385 mg, 1.25 mmol) gave **2d** (633 mg, 79.9% yield) as a brick-red solid. The complex was dissolved in CH_2Cl_2 at room temperature, and then slow diffusion under an atmosphere of nitrogen over one week gave crystals suitable for X-ray crystallography. $\text{C}_{30}\text{H}_{26}\text{Br}_2\text{N}_2\text{NiP}_2$ (694.99): calcd. C 51.85, H 3.77, N 4.03; found

Table 4. Crystallographic data and refinement for **1f** and complexes **2a–2e**.

	1f	2a ·CH ₂ Cl ₂	2b	2c	2d ·CH ₂ Cl ₂	2e ·CH ₂ Cl ₂
Formula	C ₃₁ H ₂₈ N ₂ O ₂ P ₂	C ₃₂ H ₂₉ Br ₂ Cl ₂ NNiP ₂	C ₂₉ H ₂₅ Br ₂ NNiOP ₂	C ₂₉ H ₂₅ Br ₂ NNiP ₂ S ₁	C ₃₁ H ₂₈ Br ₂ Cl ₂ N ₂ NiP ₂	C ₃₁ H ₂₉ Br ₂ Cl ₂ N ₁ Ni ₁ P ₂ S ₁
<i>F</i> _v	522.49	778.93	683.97	700.03	779.92	798.98
Crystal system	monoclinic	monoclinic	monoclinic	orthorhombic	monoclinic	monoclinic
Space group	<i>P</i> 2 ₁ / <i>c</i>	<i>P</i> 2 ₁ / <i>n</i>	<i>P</i> 2 ₁ / <i>n</i>	<i>P</i> 2 ₁ 2 ₁ 2 ₁	<i>P</i> 2 ₁ / <i>n</i>	<i>P</i> 2 ₁ / <i>n</i>
<i>a</i> [Å]	13.1615(17)	11.1913(11)	8.9824(14)	8.791(2)	9.8374(16)	11.2597(12)
<i>b</i> [Å]	18.721(3)	18.3357(18)	21.020(3)	15.901(4)	18.276(3)	16.3578(17)
<i>c</i> [Å]	11.1081(15)	15.9349(15)	14.631(2)	21.311(6)	18.292(3)	17.4648(17)
<i>α</i> [°]	90	90	90	90	90	90
<i>β</i> [°]	101.545(2)	94.252(2)	94.249(3)	90	98.537(3)	92.537(2)
<i>γ</i> [°]	90	90	90	90	90	90
<i>V</i> [Å ³]	2681.7(6)	3260.8(5)	2754.9(7)	2978.8(13)	3252.2(9)	3213.6(6)
<i>Z</i>	4	4	4	4	4	4
<i>D</i> _{calcd.} [g cm ^{−3}]	1.294	1.587	1.649	1.561	1.593	1.651
<i>μ</i> [mm ^{−1}]	0.194	3.331	3.745	3.530	3.340	3.444
<i>F</i> (000)	1096	1560	1368	1400	1560	1600
Cryst. size [mm]	0.50 × 0.42 × 0.32	0.12 × 0.08 × 0.05	0.09 × 0.06 × 0.05	0.10 × 0.08 × 0.04	0.12 × 0.07 × 0.06	0.10 × 0.06 × 0.04
<i>θ</i> [°]	1.58–26.05	1.70–26.00	1.70–27.07	1.91–26.04	1.58–26.00	1.71–26.00
No. of data collected	12450	20163	18431	14298	17753	17480
No. of unique data	5266	6393	6045	5815	6376	6304
<i>R</i> _{int}	<i>R</i> _{int} = 0.0222	<i>R</i> _{int} = 0.0468	<i>R</i> _{int} = 0.0390	<i>R</i> _{int} = 0.0499	<i>R</i> _{int} = 0.0549	<i>R</i> _{int} = 0.0402
GOF on <i>F</i> ²	1.046	1.030	1.015	1.067	1.025	1.020
Final <i>R</i> indexes	<i>R</i> ₁ = 0.0500	<i>R</i> ₁ = 0.0383	<i>R</i> ₁ = 0.0328	<i>R</i> ₁ = 0.0425	<i>R</i> ₁ = 0.0411	<i>R</i> ₁ = 0.0327
[<i>I</i> > 2σ(<i>I</i>)]	<i>wR</i> ₂ = 0.1257	<i>wR</i> ₂ = 0.0979	<i>wR</i> ₂ = 0.0770	<i>wR</i> ₂ = 0.1104	<i>wR</i> ₂ = 0.0947	<i>wR</i> ₂ = 0.0767
<i>R</i> indexes (all data)	<i>R</i> ₁ = 0.0683	<i>R</i> ₁ = 0.0583	<i>R</i> ₁ = 0.0617	<i>R</i> ₁ = 0.0571	<i>R</i> ₁ = 0.0817	<i>R</i> ₁ = 0.0522
	<i>wR</i> ₂ = 0.1400	<i>wR</i> ₂ = 0.1113	<i>wR</i> ₂ = 0.0887	<i>wR</i> ₂ = 0.1188	<i>wR</i> ₂ = 0.1197	<i>wR</i> ₂ = 0.0868

C 52.10, H 3.79, N 4.05. ¹H NMR (400 MHz CDCl₃): δ = 8.00–7.94 (m, 9 H), 7.63–7.58 (m, 4 H), 7.50–7.45 (m, 8 H), 7.24–7.20 (t, 1 H), 6.94–6.91 (t, 1 H), 6.17–6.14 (d, 1 H), 4.03–3.98 (t, 2 H) ppm. ³¹P NMR (161.97 MHz, CDCl₃): δ = 52.33 (s) ppm.

C₄H₃SCH₂CH₂N(PPh₂)₂NiBr₂ (2e): By using a similar method as adopted above, a mixture of **1e** (480 mg, 0.97 mmol) and (DME)-NiBr₂ (328 mg, 1.07 mmol) gave **2e** (585 mg, 84.5% yield) as a brick-red solid. The complex was dissolved in CH₂Cl₂/hexane at room temperature, and then slow diffusion under an atmosphere of nitrogen over one week gave crystals suitable for X-ray crystallography. C₃₀H₂₇Br₂NNiP₂S (714.06): calcd. C 50.46, H 3.81, N 1.96; found C 50.68, H 3.91, N 1.85. ¹H NMR (400 MHz, CDCl₃): δ = 8.04–7.99 (m, 8 H), 7.70–7.66 (t, 4 H), 7.60–7.56 (t, 8 H), 7.02–7.00 (d, 1 H), 6.77–6.75 (t, 1 H), 6.39–6.38 (d, 1 H), 3.05–2.94 (m, 2 H), 2.37–2.32 (m, 2 H) ppm. ³¹P NMR (161.97 MHz, CDCl₃): δ = 48.85 (s) ppm.

Ethylene Oligomerization: The oligomerization under 0.5 atm of ethylene was carried out in a typical procedure as follows. A 50-mL flask was back-filled twice with ethylene, the proper amount of MAO or Et₂AlCl was added, and then freshly distilled toluene (30 mL) was added by syringe under an ethylene atmosphere at the desired oligomerization temperature. The resulting mixtures were stirred for a further 5 min, and the catalyst precursor in CH₂Cl₂ was injected by syringe. The reaction solution was vigorously stirred under 0.5 atm of ethylene for the desired time. The flask was cooled to 0 °C and then quenched with H₂O (5 mL). About 2 mL organic solution was dried with anhydrous Na₂SO₄ for GC–MS analysis.

X-ray Structure Determination: The crystals were mounted on a glass fiber by using the oil drop scan method. Dates obtained with the ω-2θ scan mode were collected with a Bruker SMART 1000 CCD diffractometer with graphite-monochromated Mo-*K*_α radiation (λ = 0.71073 Å). The structures were solved by direct methods, whereas further refinement with full-matrix least-squares on *F*² was

obtained with the SHELXTL program package. All non-hydrogen atoms were refined anisotropically. Hydrogen atoms were introduced in calculated positions with the displacement factor of the host carbon atoms. The unit cells of **2a**, **2d**, and **2e** were found to contain one free solvent molecule. Crystal data and processing parameters for **1f** and complexes **2a–e** are summarized in Table 4.

CCDC-723879 (for **1f**), -723880 (for **2a**), -723881 (for **2b**), -723882 (for **2c**), -723883 (for **2d**), and -723884 (for **2e**) contain the supplementary crystallographic data for this paper. These data can be obtained free of charge from the Cambridge Crystallographic Data Centre via www.ccdc.cam.ac.uk/data_request/cif.

Acknowledgments

Financial support of the National Natural Science foundation of China (NSFC) (Projects 20604034, 20674097, and 20734004), the Guangdong Natural Science Foundation (NSFG) (Projects 8251027501000018 and 06300069), and the Ministry of Education of China (Foundation for PhD Training) are gratefully acknowledged. We thank Dr. Wei-xiong Zhang for single-crystal X-ray technical assistance.

- [1] J. Skupinska, *Chem. Rev.* **1991**, *91*, 613–648.
- [2] a) W. Keim, F. H. Kowaldt, R. Goddard, C. Krüger, *Angew. Chem. Int. Ed. Engl.* **1978**, *17*, 466–467; b) W. Keim, A. Behr, B. Limbäcker, C. Krüger, *Angew. Chem. Int. Ed. Engl.* **1983**, *22*, 503; c) W. Keim, A. Behr, B. Gruber, B. Hoffmann, F. H. Kowaldt, U. Kürschner, B. Limbäcker, F. P. Sisti, *Organometallics* **1986**, *5*, 2356–2359; d) W. Keim, *Angew. Chem. Int. Ed. Engl.* **1990**, *29*, 235–244.
- [3] a) S. D. Ittel, L. K. Johnson, M. Brookhart, *Chem. Rev.* **2000**, *100*, 1169–1203; b) C. M. Killian, L. K. Johnson, M. Brookhart, *Organometallics* **1997**, *16*, 2005–2007; c) S. A. Svejda, M. Brookhart, *Organometallics* **1999**, *18*, 65–74.

- [4] a) P. Kuhn, D. Smeril, C. Jeunesse, D. Matt, M. Neuburger, A. Mota, *Chem. Eur. J.* **2006**, *12*, 5210–5219; b) P. Kuhn, D. Smeril, D. Matt, M. J. Chetcuti, P. Lutz, *Dalton Trans.* **2007**, 515–528; c) P. Kuhn, D. Smeril, C. Jeunesse, D. Matt, P. Lutz, R. Welter, *Eur. J. Inorg. Chem.* **2005**, 1477–1481; d) J. Heinicke, M. Köhler, N. Peulecke, M. He, M. K. Kindermann, W. Keim, G. Fink, *Chem. Eur. J.* **2003**, *9*, 6093–6107; e) J. M. Malinoski, M. Brookhart, *Organometallics* **2003**, *22*, 5324–5335; f) J. Heinicke, M. He, A. Dal, H. F. Klein, O. Hetche, W. Keim, U. Flörke, H. J. Haupt, *Eur. J. Inorg. Chem.* **2000**, 431–440.
- [5] a) F. Speiser, P. Braunstein, L. Saussine, *Acc. Chem. Res.* **2005**, *38*, 784–793; b) A. Kermagoret, P. Braunstein, *Organometallics* **2008**, *27*, 88–99.
- [6] a) L.-C. Liang, P.-S. Chien, P.-Y. Lee, *Organometallics* **2008**, *27*, 3082–3093; b) I. Albers, E. Alvarez, J. Campora, C. M. Maya, P. Palma, L. J. Sanchez, E. Passaglia, *J. Organomet. Chem.* **2004**, *689*, 833–839.
- [7] a) T. Appleby, J. D. Woollins, *Coord. Chem. Rev.* **2002**, *235*, 121–140; b) Z. Fei, P. J. Dyson, *Coord. Chem. Rev.* **2005**, *249*, 2056–2074.
- [8] a) K. G. Gaw, M. B. Smith, A. M. Z. Slawin, *New J. Chem.* **2000**, *24*, 429–435; b) I. Bachert, I. Bartussek, P. Braunstein, E. Guillon, J. Rosé, G. Kickelbick, *J. Organomet. Chem.* **1999**, *580*, 257–264.
- [9] a) A. Carter, S. A. Cohen, N. A. Cooley, A. Murphy, J. Scutt, D. F. Wass, *Chem. Commun.* **2002**, 858–859; b) A. Bollmann, K. Blann, J. T. Dixon, F. M. Hess, E. Killian, H. Maumela, D. S. McGuinness, D. H. Morgan, A. Neveling, S. Otto, M. Overett, A. M. Z. Slawin, P. Wasserscheid, S. Kuhlmann, *J. Am. Chem. Soc.* **2004**, *126*, 14712–14713; c) D. F. Wass, *Dalton Trans.* **2007**, 816–819; d) S. Kuhlmann, K. Blann, A. Bollmann, J. T. Dixon, E. Killian, M. C. Maumela, H. Maumela, D. H. Morgan, M. Prétorius, N. Taccardi, P. Wasserscheid, *J. Catal.* **2007**, *245*, 279–284; e) T. Agapie, S. J. Schofer, J. A. Labinger, J. E. Bercaw, *J. Am. Chem. Soc.* **2004**, *126*, 1304–1305.
- [10] a) N. A. Cooley, S. M. Green, D. F. Wass, *Organometallics* **2001**, *20*, 4769–4771; b) L. Lavanant, A.-S. Rodrigues, E. Kirillov, J.-F. Carpentier, R. F. Jordan, *Organometallics* **2008**, *27*, 2107–2117.
- [11] N. L. Dennett, A. L. Gillon, K. Heslop, D. J. Hyett, J. S. Fleming, C. E. Lloyd-Jones, A. G. Orpen, P. G. Pringle, D. F. Wass, *Organometallics* **2004**, *23*, 6077–6079.
- [12] P. R. Elowe, C. McCann, P. G. Pringle, S. K. Spitzmesser, J. E. Bercaw, *Organometallics* **2006**, *25*, 5255–5260.
- [13] Z. Weng, S. Teo, T. S. A. Hor, *Dalton Trans.* **2007**, 3493–3498.
- [14] a) D. J. Jone, V. C. Gibson, S. Green, P. Maddox, *Chem. Commun.* **2002**, 1038–1039; b) D. C. H. Oakes, B. S. Kimberley, V. C. Gibson, D. J. Jones, A. J. P. White, D. Williams, *Chem. Commun.* **2004**, 2174–2175; c) C. Wang, Z. Ma, X.-L. Sun, Y. Gao, Y.-H. Guo, Y. Tang, L.-P. Shi, *Organometallics* **2006**, *25*, 3259–3266; d) W.-F. Li, W.-H. Sun, G.-M. Chen, G.-Z. Wang, M.-D. Hu, Q. Shen, Y. Zhang, *Organometallics* **2005**, *24*, 5925–5928; e) V. Lozan, P. G. Lassahn, C. Zhang, B. Wu, C. Janiak, G. Rheinwald, H. Z. Lang, *Naturforsch. B* **2003**, *58*, 1152–1164; f) J. Hou, W.-H. Sun, S. Zhang, H. Ma, Y. Deng, X. Lu, *Organometallics* **2006**, *25*, 236–244; g) E. Y. Tshuva, S. Groysman, I. Godbeg, M. Kol, *Organometallics* **2002**, *21*, 662–670; h) G. Siedle, P. G. Lassahn, V. Lozan, C. Janiak, B. Kersting, *Dalton Trans.* **2007**, 52–61.
- [15] Z. Fei, R. Scopelliti, P. J. Dyson, *Dalton Trans.* **2003**, 2772–2779.
- [16] Z. Fei, D. Zhao, N. Biricik, R. Scopelliti, P. J. Dyson, *Inorg. Chem.* **2004**, *43*, 2228–2230.
- [17] Biricik, F. Durap, C. Kayan, B. Gümgüm, N. Gürbüz, I. Özdemir, W. H. Ang, Z. Fei, R. Scopelliti, *J. Organomet. Chem.* **2008**, *693*, 2693–2699.
- [18] Z.-G. Sun, F.-M. Zhu, Q. Wu, S.-A. Lin, *Appl. Organomet. Chem.* **2006**, *20*, 175–180.
- [19] a) A. M. Z. Slawin, J. Wheatley, J. D. Woollins, *Eur. J. Inorg. Chem.* **2005**, 713–720; b) Z. Fei, R. Scopelliti, P. J. Dyson, *Eur. J. Inorg. Chem.* **2003**, 3527–3529; c) Z. Fei, R. Scopelliti, P. J. Dyson, *Eur. J. Inorg. Chem.* **2004**, 530–537; d) N. Biricik, Z. Fei, R. Scopelliti, P. J. Dyson, *Eur. J. Inorg. Chem.* **2004**, 4232–4236; e) I. Fernández, F. Breher, P. S. Pregosin, Z. Fei, P. J. Dyson, *Inorg. Chem.* **2005**, *44*, 7616–7623; f) Z. Fei, R. Scopelliti, P. J. Dyson, *Inorg. Chem.* **2003**, *42*, 2125–2130.
- [20] D. F. Wass (BP Chemicals Ltd), WO 01/10876, **2001**.
- [21] a) J.-L. Huang, T.-Z. Wu, Y.-L. Qian, *Chem. Commun.* **2003**, 2816–2817; b) C. Bianchini, G. Mantovani, A. Meli, F. Migliacci, F. Laschi, *Organometallics* **2003**, *22*, 2545–2547; c) C. Bianchini, G. Giambastiani, G. Mantovani, A. Meli, D. Mimeo, *J. Organomet. Chem.* **2004**, *689*, 1356–1361; d) C. Bianchini, D. Gatteschi, G. Giambastiani, I. G. Rios, A. Ienco, F. Laschi, C. Mealli, A. Meli, L. Sorace, A. Toti, F. Vizza, *Organometallics* **2007**, *26*, 726–739.
- [22] a) L. L. de Oliveira, R. R. Campedelli, M. C. A. Kuhn, J.-F. Carpentier, O. L. Casagrande Jr, *J. Mol. Catal. A* **2008**, *288*, 58–62; b) N. Ajellal, M. C. A. Kuhn, A. D. G. Boff, M. Hörner, C. M. Thomas, J.-F. Carpentier, O. L. Casagrande Jr, *Organometallics* **2006**, *25*, 1213–1216.
- [23] a) C. Zhang, W.-H. Sun, Z.-X. Wang, *Eur. J. Inorg. Chem.* **2006**, 4895–4902; b) R. Gao, M. Zhang, T. Liang, F. Wang, W.-H. Sun, *Organometallics* **2008**, *27*, 5641–5648; c) W.-H. Sun, K. Wang, K. Wedeking, D. Zhang, S. Zhang, J. Cai, Y. Li, *Organometallics* **2007**, *26*, 4781–4790.
- [24] P. G. T. Fogg, W. Gerrard, *Solubility of Gases in Liquids*, Wiley, West Sussex, England, **1991**.
- [25] S. A. Svejda, M. Brookhart, *Organometallics* **1999**, *18*, 65–74.
- [26] a) C. Perego, P. Ingallina, *Catal. Today* **2002**, *73*, 3–22; b) R. J. Davis, *J. Catal.* **2003**, *216*, 396–405; c) L. Xiao, K. E. Johnson, R. G. Treble, *J. Mol. Catal. A* **2004**, *214*, 121–127.
- [27] P. W. Dyer, J. Fawcett, M. J. Hanton, *Organometallics* **2008**, *27*, 5082–5087.
- [28] a) G. Busca, *Chem. Rev.* **2007**, *107*, 5366–5410; b) A. Corma, H. Garcia, *Chem. Rev.* **2003**, *103*, 4307–4365.
- [29] W. X. Hart, Doctoral Dissertation, University of Massachusetts, **1981**.

Received: March 18, 2009
Published Online: June 5, 2009